Supplementary material

Cell lines

MC38 cells and 4T1 cells were provided by Carlotta Tacconi and Michael Detmar (Institute of Pharmaceutical Sciences, ETH, Zurich, Switzerland), respectively. Lewis Lung carcinoma (LLC) and CT26 colon carcinoma cells were purchased from ATCC. LLC cells were lentivirally transduced to express firefly luciferase or cGAS to generate LLC-LUC or LLC-cGAS (Schadt et al., 2019) cells, respectively. Viral particles were a gift from Christian Münz (University of Zurich). All cancer cells were cultured in Dulbecco's modified Eagle's medium (DMEM, GIBCO) supplemented with 10% fetal calf serum (FCS, ThermoFisher Scientific), 30 U/ml Penicillin, 30 µg/ml Streptomycin (antibiotics, ThermoFisher Scientific) and 2mM L-Glutamine (ThermoFisher Scientific). All cancer cell lines were used between passages 2 and 10. Cell lines were confirmed to be free of *Mycoplasma* ssp. by PCR and various viruses by Charles River Research Animal Diagnostic Services.

Antibody list

CD115-Biotin (AFS98; BioLegend), CD19-Biotin (6D5; BioLegend), CD3e-Biotin (145-2C11; BioLegend), CD5-Biotin (53-7.3; BioLegend), Ly6G-Biotin (1A8; BioLegend), NK1.1-FITC (PK136; BioLegend), NK1.1-BV711 (PK136; BioLegend), NK1.1-BV785 (PK136; BioLegend), NKp46-PerCP-eFluor710 (29A1.4; eBioscience), NKp46-FITC (29A1.4; eBioscience), CD4-BV785 (104 (SJL); BioLegend), CD45-APC-Cy7 (30-F11, BioLegend), CD49a-BV510 (Ha31/8; BD Biosciences), CD49a-BUV395 (Ha31/8; BD Biosciences), CD49b-PB (DX5; BioLegend), CD27-PE (LG.3A10; BioLegend), CD27-PE-Cy7 (LG.3A10; BioLegend), CD62L-BUV737 (MEL-14; BD Biosciences), CD69-BV605 (H1.2F3; BioLegend), Thy1.2-BV785 (30-H12; BioLegend), Thy1.2-AF700 (30-H12; BioLegend), KLRG1-BV510 (2F1/KLRG1; BioLegend), CD11b-BV711 (M1/70; BioLegend), CD11b-BUV737 (M1/70; BioLegend), Ly49G2-PerCP-eFluor710 (4D11; eBioscience), EOMES-PE-texRed (Dan11mag; eBioscience), GrzB-AF647 (GB11; BioLegend), Ki67-PerCP-eFluor710 (SolA15; eBioscience), Tbet-PE-Cy7 (4B10; BioLegend), IFN-γ-PE-Cy7 (XMG1.2; BioLegend), CD107a-APC (1D4B; BioLegend),

CD8a-BV605 (53-6.7; Biolegend), Ly6G-BUV563 (1A8, BD Biosciences), Ly6C-BV711 (HK1.4, Biolegend), XCR-1-BV650 (ZET, Biolegend), CD64-BV421 (10.1, Biolegend), I-A/I-E-AF488 (M5/114.15.2, Biolegend), F4/80-PECy5 (BM8, Biolegend), CD103-PE (2E7, Biolegend), CD206-AF700 (MR6F3, eBioscience), Streptavidin-APC (BD Biosciences), Streptavidin-BUV563 (BD Biosciences), Zombie NIR™ Fixable Viability Kit (BioLegend), Zombie UV™ Fixable Viability Kit (BioLegend).

Primer list

Pol2 5'-CTTCCGGGGCCATGTATCTT-3' 5'-GCTCGATACCCTGCAGGGTCA-3'; *Il15* 5'-GTGACTTTCATCCCAGTTGC-3' 5'-TCACATTCCTTGCAGCCAGA-3'; *Il15ra* 5'-GAGGTCAGGAAAGAATCCACCT-3' 5'-AGCAAGGACCATGAAGAGGC-3'; *Il12* 5'-GAGGACTTGAAGATGTACCAG-3' 5'-TTCTATCTGTGTGAGGAGGGC-3'; *Il18* 5'-CAAACCTTCCAAATCACTTCCT-3' 5'-TCCTTGAAGTTGACGCAAGA-3'; *Ifng* 5'-GCATTCATGAGTATTGCCAAG-3' 5'-GGTGGACCACTCGGATGA-3'; *Tgfbr2* 5'-AACGACTTGACCTGTTGCCTGT-3' 5'-CTTCCGGGGCCATGTATCTT-3'; *Gzmb* 5'-ACACCTCCTTCCTCCCCTTC-3' 5'-TAGGGACGGGAATGTGGACT-3'; *Tgfb1* 5'-ATGCTAAAGAGGTCACCCGC-3' 5'-TGCTTCCCGAATGTCTGACG-3'; *Runx3* 5'-TACCTACCACCGAGCCATCA-3' 5'-TTCTATCTTCTGCCGGTGCC-3'; *Smad7* 5'-TCAAACCAACTGCAGGCTGTC-3' 5'-TCTTCTCCTCCCAGTATGCCA-3'; *Itga1* 5'-CCACCAAGATGAACGAGCCT-3' 5'-GGCTGCCCAGCGATATAGAG-3'; *Xcl1* 5'-TGAACTTACAAACCCAGCGG-3' 5'-TCGCTGCTTTCACCCATTTG-3'; *Cdk6* 5'-TCCTGCTCCAGTCCAGCTAT-3' 5'-CCACGTCTGAACTTCCACGA-3'; *Cotl1* 5'-ATCACATGGATCGGGGAGGA-3' 5'-TCCGGTCGCTGATCACAAAT-3'; *Car2* 5'-ACTGGGGATACAGCAAGCAC-3' 5'-TGCTCTTGGACGCAGCTTTA-3'; *Pmepa1* 5'-TCCTTCATCAGCCGACACAG-3' 5'-CCACCTGACACCGTACTCTC-3'.

Single-cell RNA sequencing using 10x Genomics platform

NKp46$^+$ cells (live CD45$^+$CD3$^-$CD5$^-$Ly6G$^-$CD19$^-$CD115$^-$NK1.1$^+$NKp46$^+$) were sorted from naïve, LLC and MC38 metastatic livers. For each sample, cells were pooled from 6 biological replicates. The quality and concentration of the single cell preparations were evaluated using an hemocytometer in a Leica MD IL LED microscope and adjusted to 1'000 cells/ml. 10'000 cells per sample were loaded in to the 10X Chromium controller and library preparation

was performed according to the manufacturer's indications (Chromium Next GEM Single Cell 3' Reagent Kits v3 protocol). The resulting libraries were sequenced in an Illumina NovaSeq6000 sequencer according to 10X Genomics recommendations (paired-end reads, R1=28, i7=8, R2=91) to a depth of around 50,000 reads per cell. FASTQ files were created with the Cell Ranger demux pipeline. Reads were pseudo-aligned to a mouse reference (ensemble release 97) with the kallisto/bus pipeline (https://www.kallistobus.tools/velocity_tutorial.html), using kallisto v0.46.0 (ref PMID: 27043002) and bustools v0.39.3 (ref PMID: 31073610). The resulting count matrix was analyzed with Seurat v3 (ref PMID: 31178118). Data were scaled and transformed using SCTransform v0.2.0 (ref PMID: 31870423) for variance stabilization. The experiment resulted in the following number of obtained cells: 9164 cells from naïve livers (median of 1543 unique genes detected per cell), 8910 cells from LLC metastatic livers (median of 1681 unique genes detected per cell), and 9565 cells from MC38 metastatic livers (median of 1606 unique genes detected per cell). Contaminating cell clusters that were NKp46 negative and did not consist of NK cells were excluded from further analyses. Principle Component Analysis was performed on the expression of the detected variable genes. The first 50 principal components were included for further downstream analyses based on visual inspection of Seurat's PCElbowPlot. All cells were clustered based on the principal component analysis with the Louvain algorithm using the following granularity parameters: resolution = 0.5. Differential marker expression analyses were conducted with the Seurat FindMarkers and FindAllMarkers functions. 10x libraries were prepared and sequenced at the Functional Genomics Center (University of Zürich).

Gene ontology analysis

Gene Ontology (GO) analysis was performed with EnrichR (Chen et al., 2013). Venn diagrams were created using the jvenn online tool (Bardou et al., 2014).

Supplementary Figure 1. Absence of NKp46⁺ cells, CD8⁺ T cells, cNKs or trILC1s in different experimental systems, and resulting effect on hepatic metastatic load.

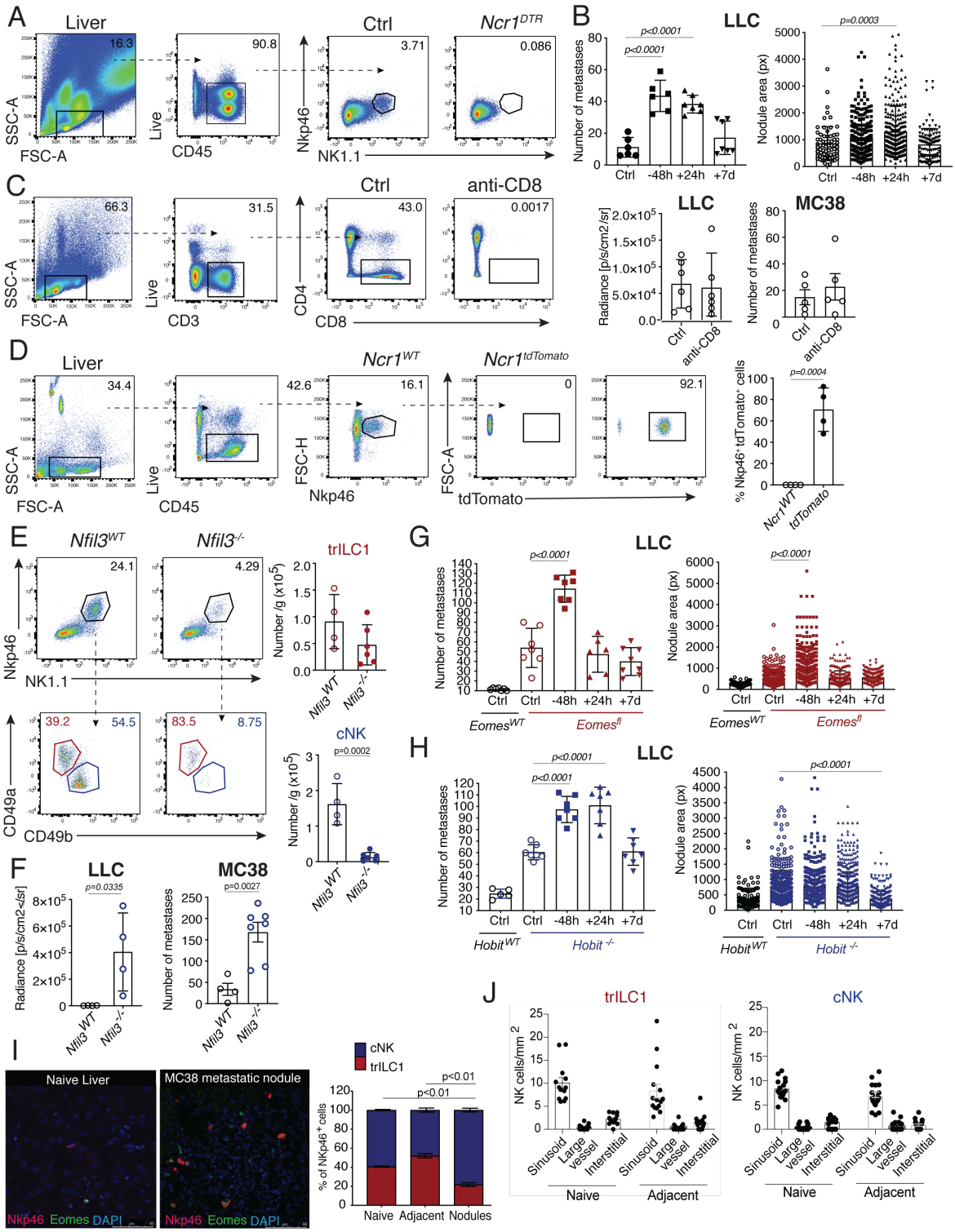

Supplementary Figure 1. Absence of NKp46$^+$ cells, CD8$^+$ T cells, cNKs or trILC1s in different experimental systems, and resulting effect on hepatic metastatic load.

(A) NKp46$^+$ cells were depleted by injection of 250 ng diphtheria toxin intraperitoneally as indicated in Figure 1A. Representative detection of NKp46$^+$ cells in livers of control mice (*Ncr1*$^{iCre/wt}$*R26R*$^{wt/wt}$) and *Ncr1*^{DTR} (*Ncr1*$^{iiCre/wt}$*. R26R*$^{iDTR/wt}$) at the endpoint. **(B)** NKp46$^+$ cells were depleted by injection of 250 ng diphtheria toxin intraperitoneally 48 hours before, 24 hours after or 7 days after tumor injection. Depletion was maintained until the endpoint. *Ncr1*^{DTR} = *Ncr1*$^{iCre/wt}$*.R26R*$^{iDTR/wt}$; Ctrl = undepleted control mice (*Ncr1*$^{iCre/wt}$*.R26R*$^{wt/wt}$, group injected at time point -48h). Panels: Quantification of LLC macroscopic liver nodules and their area at the endpoint. The bar represents the mean ± SD, symbols represent livers from individual mice. Each dot in the nodule area represents an individual metastatic nodule. One-way analysis of variance (ANOVA), with Tukey's multiple comparisons test. The experiment was performed twice with similar results. **(C)** CD8$^+$ T cells were depleted by i.p. injection of 100 µg anti-CD8 (anti-CD8) or isotype control (Ctrl) antibody at -48 h relatively to tumor cell injection. Dot plots: Representative detection of CD8$^+$ T cells depletion in blood of C57BL/6 mice. Bar graphs: Quantification of LLC liver nodules by *ex vivo* IVIS imaging or MC38 macroscopic liver nodules at the endpoint. The bar represents the mean ± SD, symbols represent livers from individual mice, groups consisted of 5-6 mice. One-way analysis of variance (ANOVA), with Tukey's multiple comparisons test. The experiment was performed twice with similar results. **(D)** Representative dot plots and quantification of NKp46$^+$ cell in naive livers of *Ncr1*^{WT} = *Ncr1*$^{iCre/wt}$*.R26R*$^{wt/wt}$; *Ncr1*^{tdTomato} = *Ncr1*$^{iCre/wt}$*.R26R*$^{Ai14/wt}$ mice. The bar represents the mean ± SD, symbols represent livers from individual mice. Unpaired Student's t-test. Pooled data from two experiments are shown. **(E)** Representative dot plots and quantification of cNKs and trILC1s in naïve livers of *Nfil3*^{WT} and *Nfil3*$^{-/-}$ mice. Samples were pre-gated on single live CD45$^+$lineage$^-$ cells and subsequently gated on NK1.1$^+$NKp46$^+$ cells. cNK = conventional NK cells, CD49a$^-$CD49b$^+$; trILC1 = tissue-resident ILC1s, CD49a$^+$CD49b$^-$. The bar represents the mean ± SD, symbols represent livers from individual mice, groups consisted of 4-6 mice. Student's unpaired t test. The experiment was performed twice with similar results. **(F)** Quantification of the LLC- and MC38-derived metastatic burden in livers of *Nfil3*^{WT} and *Nfil3*$^{-/-}$ mice as described under (C). The bar represents the mean ± SD, symbols represent livers from individual mice, groups consisted of 4-7 mice. Unpaired Student's t-test. The experiment was performed twice with similar results. **(G)** trILC1s were depleted by injection of 250 ng diphtheria toxin intraperitoneally 48 hours before, 24 hours after or 7 days after tumor injection. Depletion was maintained until the endpoint (day 18). *Eomes*^{WT} Ctrl = *Ncr1*$^{iCre/wt}$*.Eomes*$^{wt/wt}$*.R26R*$^{wt/wt}$; *Eomes*^{fl} Ctrl = *Ncr1*$^{iCre/wt}$*.Eomes*$^{fl/fl}$*.R26R*$^{wt/wt}$; *Eomes*^{fl} NKp46$^+$-depleted = *Ncr1*$^{iCre/wt}$*.Eomes*$^{fl/fl}$*.R26R*$^{iDTR/wt}$. Panels: Quantification of liver nodules and their area at endpoint. The bar represents the mean ± SD, symbols represent livers from individual mice. Each dot in the nodule area represents an individual metastatic nodule. One-way analysis of variance (ANOVA), with Tukey's multiple comparisons test. The experiment was performed twice with similar results. **(H)** Depletion of cNK cells in *Hobit*^{WT} and *Hobit*$^{-/-}$ mice using anti-Asialo-GM1. Depletion was started 48 hours before, 24 hours after or 7 days after tumor injection, and maintained until the endpoint (day 18). Panels: Quantification of liver nodules and their area at endpoint. The bar represents the mean ± SD, symbols represent livers from individual mice. Each dot in the nodule area represents an individual metastatic nodule. One-way analysis of variance (ANOVA), with Tukey's multiple comparisons test. The experiment was performed twice with similar results. **(I**) Left two panels: Representative immunofluorescence images of a naïve and a MC38-metastatic liver from *Ncr1*$^{iCre/wt}$*.R26R*$^{Ai14/wt}$ wt mice. Right panel: quantification of the localization of cNKs and trILC1s in naïve livers, adjacent tissue to the nodule and metastatic nodules. Four naïve and four MC38-metastatic livers were analyzed and the results are expressed in % of trILC1s or cNKs versus total. One-way analysis of variance (ANOVA), with Tukey's multiple comparisons test. **(J**) Quantification of the vascular localization of trILC1s and cNK cells using *Ncr1*$^{iCre/wt}$*.Eomes*$^{fl/fl}$*.R26R*$^{Ai14/wt}$ mice and *Ncr1*$^{iCre/wt}$*.Hobit*$^{-/-}$*.R26R*$^{Ai14/wt}$ mice in naïve liver or in the adjacent tissue of MC38-metastatic liver. Three livers per experimental condition were analyzed, each symbol represents an individual section. The distribution of trILC1s and cNK cells was determined based on their positioning relative to liver vasculature (associated to the sinusoids or large vessels, or interstitial).

Supplementary Figure 2. Multi-parameter single-cell mapping of cNKs and trlLC1s cells in blood and livers from naïve and metastatic mice.

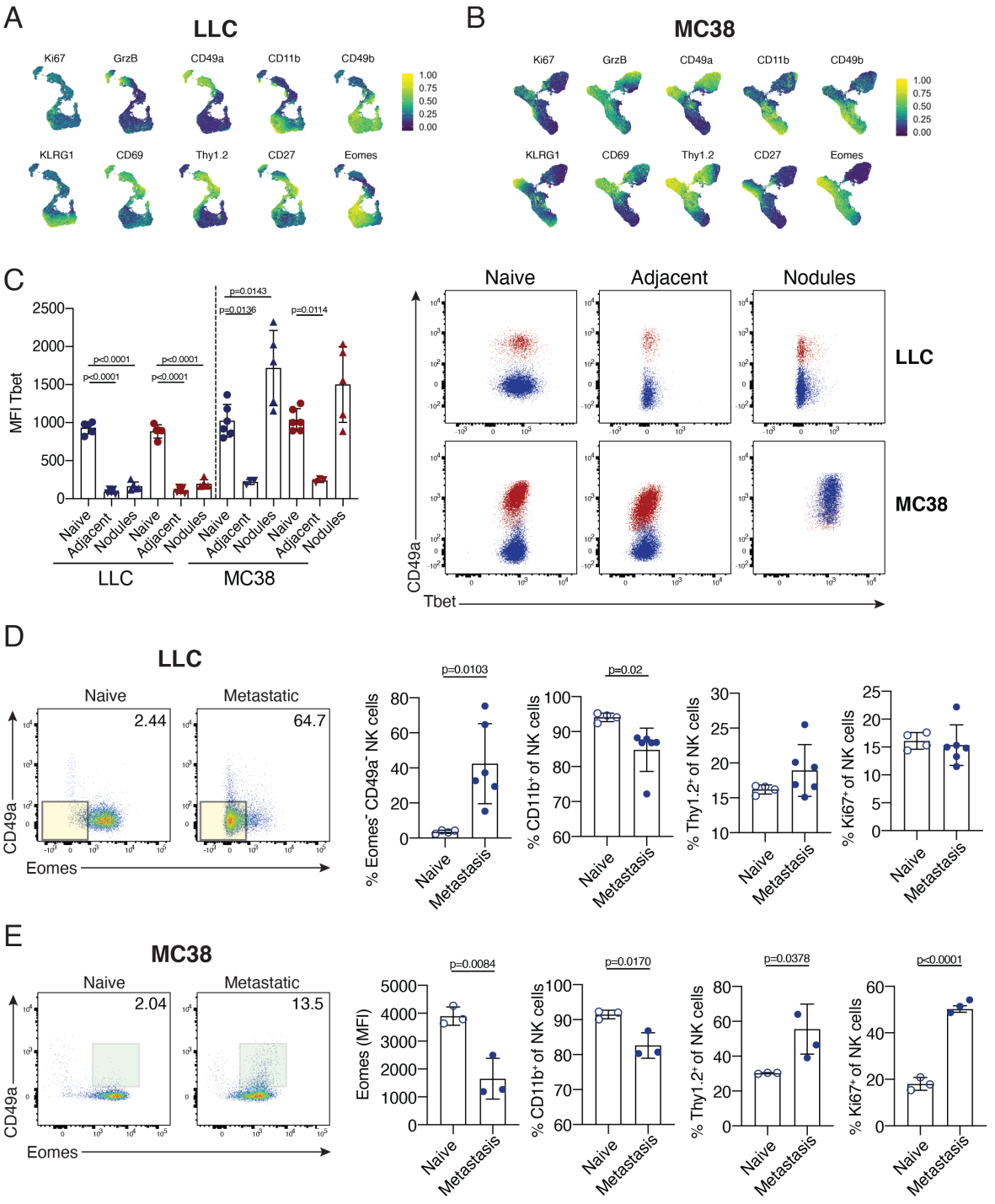

Supplementary Figure 2. Multi-parameter single-cell mapping of cNKs and trILC1s cells in blood and livers from naïve and metastatic mice.

Naïve and metastatic livers were collected. Metastatic livers (day 21) were manually dissected to separate the nodules from the adjacent tissue, and tissues were enzymatically processed into a single-cell suspension. NKp46^{+} cells were analyzed by multi-parameter single-cell mapping using flow cytometry. UMAP visualization of markers after gating on single, live, CD45^{+}lin^{-}NK1.1^{+}NKp46^{+}cells. **(A)** LLC-metastatic livers. **(B)** MC38-metastatic livers. **(C)** Expression of Tbet by cNKs (blue) and trILC1s (red) in metastatic livers. The bar represents the mean ± SD, symbols represent livers from individual mice, groups consisted of 3-5 mice. One-way analysis of variance (ANOVA), with Tukey's multiple comparisons test. The experiment was performed twice with similar results. **(D)** Flow cytometry analysis of CD49a^{-}Eomes^{-} population from blood of mice with naïve or LLC-metastatic livers. Left panels: Highlighted in yellow is the CD49a^{-}Eomes^{-} population. Right panels: Quantification of CD49a^{-} Eomes^{-} population, CD11b^{+}, Thy1.2^{+} and Ki67^{+} cells in cNKs (blue). The bar represents the mean ± SD, symbols represent livers from individual mice, groups consisted of 4-5 mice. Unpaired Student's t-test. The experiment was performed twice with similar results. **(E)** Flow cytometry analysis of CD49a^{+}Eomes^{+} population from blood of mice with naïve or MC38-metastatic livers. Left panels: Highlighted in green is the CD49a^{+}Eomes^{+} population. Right panels: Quantification of Eomes expression, CD11b^{+}, Thy1.2^{+} and Ki67^{+} cells in cNKs. The bar represents the mean ± SD, symbols represent livers from individual mice, groups consisted of 3 mice. Unpaired Student's t-test. The experiment was performed twice with similar results.

Supplementary Figure 3. Metastasis drives the emergence of unique cNK cell populations.

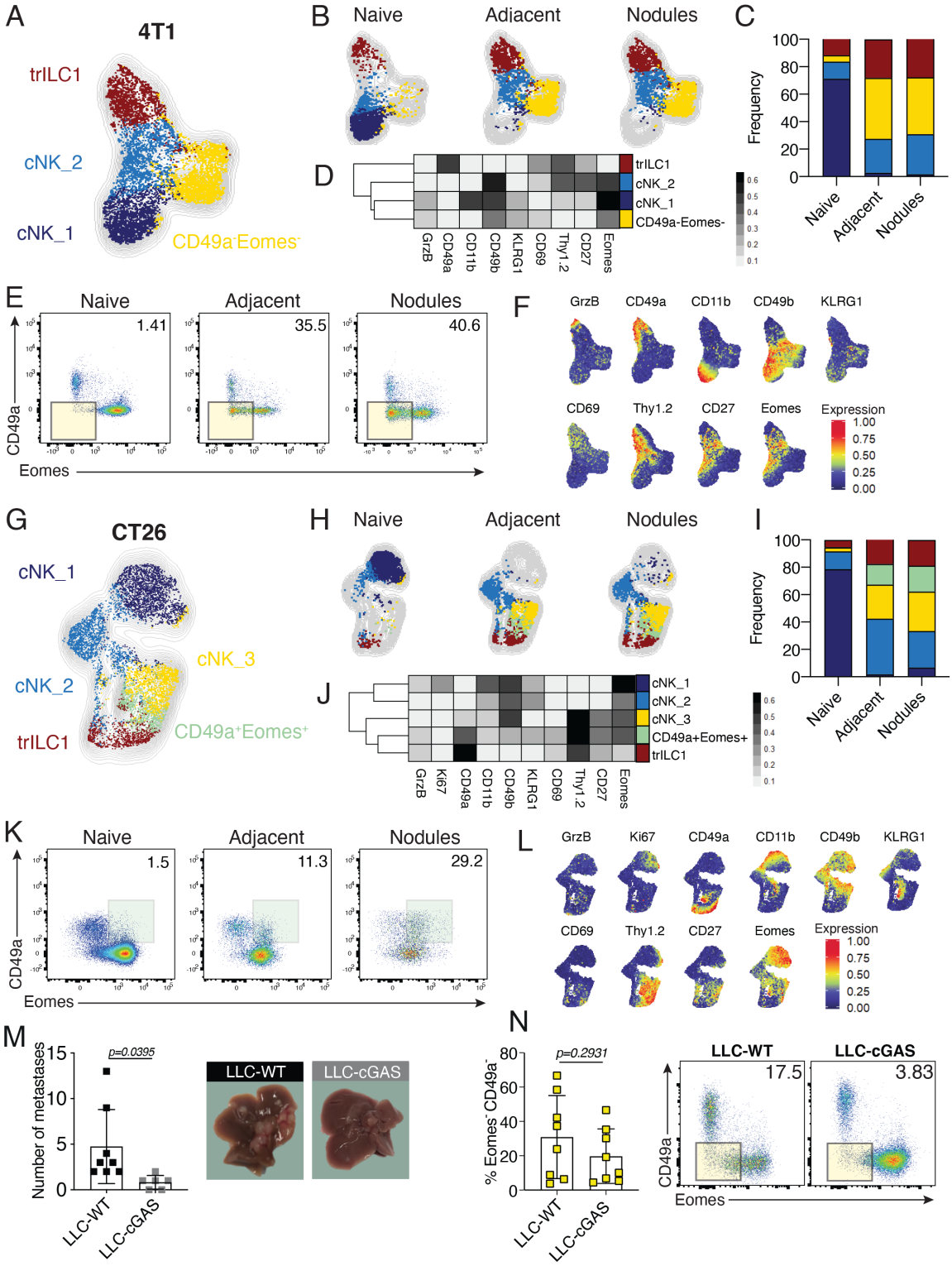

Supplementary Figure 3. Metastasis drives the emergence of unique cNK cell populations.

Naïve and metastatic livers were collected. Metastatic livers (day 21) were manually dissected to separate the nodules from the adjacent tissue, and tissues were enzymatically processed into a single-cell suspension. NKp46^{+} cells were analyzed by multi-parameter single-cell mapping using flow cytometry. Samples were pre-gated on single live CD45^{+}lineage^{-} cells and subsequently gated on NK1.1^{+}NKp46^{+} cells. cNK = conventional NK cells, CD49a^{-}CD49b^{+}; trILC1 = tissue-resident ILC1s, CD49a^{+}CD49b^{-}. **(A-F)** 4T1-metastatic and control livers. **(G-L)** CT26-metastatic and control livers. **(A, G)** UMAP maps overlaid with FlowSOM-guided manual metaclusters displaying cNKs and trILC1s from all samples. **(B, H)** UMAP maps overlaid with FlowSOM-guided manual metaclusters separated by sample category (naïve, adjacent, nodules). **(C, I)** Relative frequency of each cluster in the different sample categories (naïve, adjacent, nodules). **(D, J)** Heatmap summary of median marker expression values of the different markers analyzed for each cluster. **(E)** Highlighted in yellow is the CD49a^{-}Eomes^{-} population observed in 4T1 adjacent tissue and nodules. **(F)** UMAP visualization of markers after gating on single, live, CD45^{+}lin^{-}NK1.1^{+}NKp46^{+}cells. **(K)** Highlighted in green is the CD49a^{+}Eomes^{+} population observed in CT26 nodules. **(L)** UMAP visualization of markers after gating on single, live, CD45^{+}lin^{-}NK1.1^{+}NKp46^{+} cells in mice. Experimental groups consisted of 4-5 mice. The experiment was performed twice with similar results. **(M)** Left panel: Macroscopic quantification of LLC-WT and LLC-cGAS metastatic nodules in the liver of C57BL/6 mice 21 days after tumor cell injection. Bars show the mean ± SD. Each symbol represents an individual mouse. One-way analysis of variance (ANOVA), with Tukey's multiple comparisons test. The experiment was performed twice with similar results. Right panels: Representative images of metastatic livers from each group at the endpoint. LLC-WT = control LLC cells; LLC-cGAS = LLC cells overexpressing cGAS (*Mb21d1*). **(N)** Left panel: Percentage of CD49a^{-}Eomes^{-} NKp46^{+} cells in LLC-WT and LLC-cGAS nodules. Bars show the mean ± SD. Each symbol represents an individual mouse. One-way analysis of variance (ANOVA), with Tukey's multiple comparisons test. The experiment was performed twice with similar results. Right panel: Representative dot plots of cNKs and trILC1s in LLC-WT and LLC-cGAS nodules, with the CD49a^{-}Eomes^{-} population highlighted in yellow.

Supplementary Figure 4. Analysis of the myeloid compartment in MC38 and LLC-derived metastatic nodules. Effector functions of cNKs and trILC1s in naïve and metastatic livers after stimulation with PMA + ionomycin.

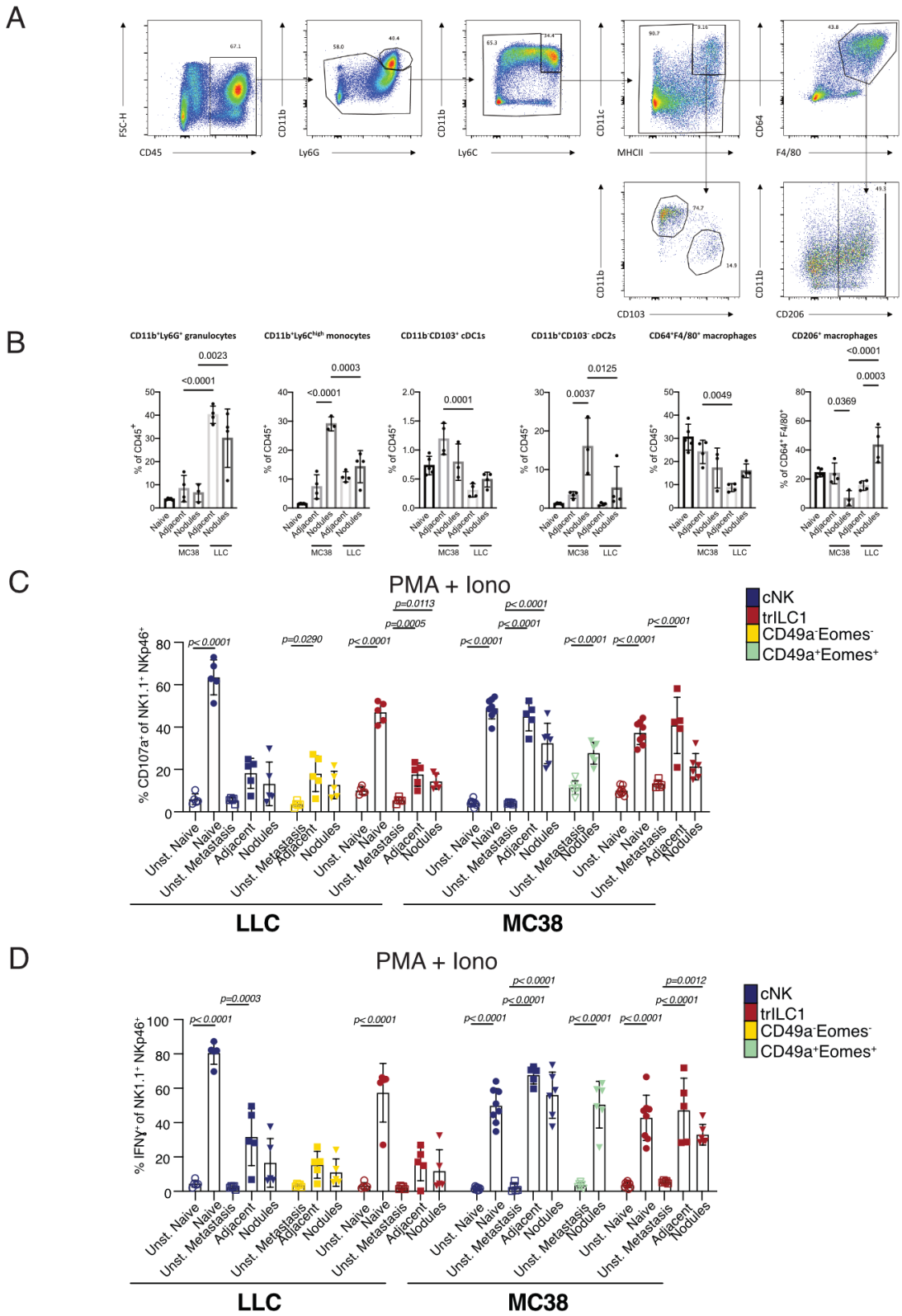

Supplementary Figure 4. Analysis of the hepatic myeloid compartment in MC38 and LLC-derived metastatic nodules. Effector functions of cNKs and trILC1s in naïve and metastatic livers after stimulation with PMA + ionomycin.

Livers from naïve mice or MC38 and LLC-derived metastases were analyzed 21 days after tumor inoculation followed by splenectomy using flow cytometry. Naïve liver was analyzed in parallel to adjacent and metastatic nodules. Livers cells were pre-gated on single cells, live cells and lineage- (lin^-) cells (CD3, B220 and NK1.1). (**A**) Representative gating strategy of the different myeloid populations for an LLC-derived metastatic nodule. (**B**) Quantification of $CD11b^+Ly6G^+$ granulocytes, $CD11b^+Ly6C^{high}$ monocytes, $CD11b^-CD103^+$ cDC1s, $CD11b^+CD103^-$ cDC2s, $CD64^+F4/80^+$ macrophages and $CD206^+$ macrophages. Statistical analysis was performed with One-way analysis of variance (ANOVA), with Tukey's multiple comparisons test.

Naïve and LLC- or MC38-derived metastatic livers were manually dissected to separate the nodules from the adjacent tissue. Tissues were enzymatically processed into a single-cell suspension. Suspensions were stimulated for 4 hours with 100 ng/ml PMA + 1 µg/ml ionomycin and the expression of effector molecules was measured by flow cytometry. Samples were pre-gated on single live $CD45^+lineage^-$ cells and subsequently gated on $NK1.1^+NKp46^+$ cells. cNK cells ($CD49a^-$ cells) were divided into $CD49b^+Eomes^{high/int}$ cells (named here cNKs and present in naïve and both LLC and MC38 metastatic livers), $CD49b^-Eomes^-$ cells (present in LLC-derived metastatic livers) and $CD49b^+Eomes^+$ cells (present in MC38-metastatic nodules). trILC1s were gated as $CD49a^+CD49b^-$ cells. **(C)** Surface expression of CD107a after 4-h stimulation with PMA + ionomycin. **(D)** Intracellular expression of IFN-γ after 4-h stimulation with with PMA + ionomycin. Unst. = unstimulated. The bar represents the mean ± SD, symbols represent livers from individual mice, groups consisted of 5-8 mice. One-way analysis of variance (ANOVA), with Tukey's multiple comparisons test. The experiment was performed twice with similar results.

Supplementary Figure 5. Effector functions of cNKs and trILC1s in naïve and metastatic livers after stimulation with IL-15 or IL-12 + IL-18.

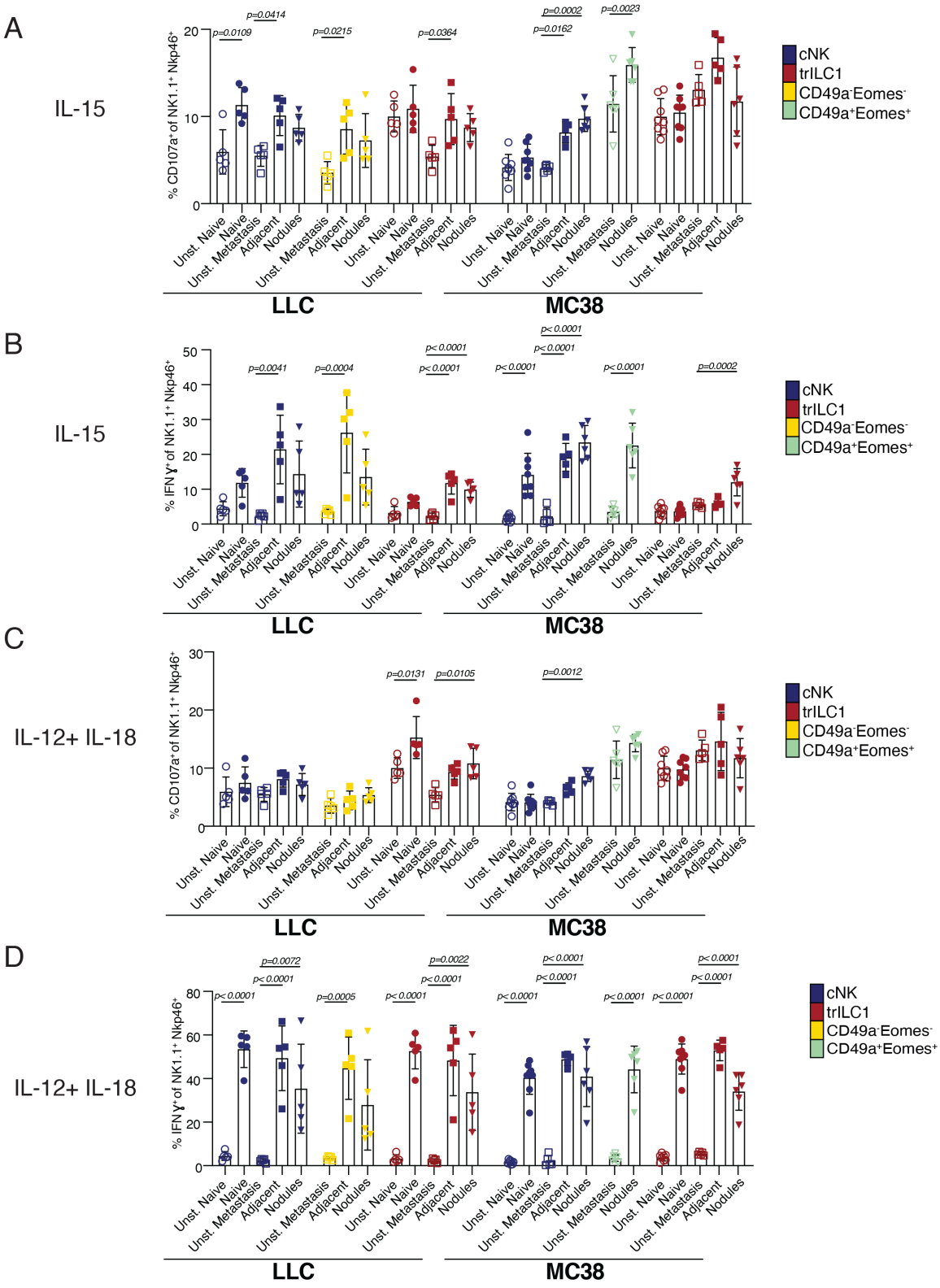

Supplementary Figure 5. Effector functions of cNKs and trILC1s in naïve and metastatic livers after stimulation with IL-15 or IL-12 + IL-18.

Naïve and metastatic livers were collected. Metastatic livers were manually dissected to separate the nodules from the adjacent tissue. Tissues were enzymatically processed into a single-cell suspension. Suspensions were stimulated for 4 hours with 10 ng/ml IL-15 **(A, B)** or 10 ng/ml IL-12 + 100 ng/ml IL-18 **(C, D)**, and the expression of effector molecules were measured by flow cytometry. Samples were pre-gated on single live $CD45^{+}$lineage^{-} cells and subsequently gated on $NK1.1^{+}NKp46^{+}$ cells. cNK cells ($CD49a^{-}$ cells) were divided into $CD49b^{+}Eomes^{high/int}$ cells (named here cNKs and present in naïve and both LLC and MC38 metastatic livers), $CD49b^{-}Eomes^{-}$ cells (present in LLC-derived metastatic livers) and $CD49b^{+}Eomes^{+}$ cells (present in MC38 nodules). trILC1s were gated as $CD49a^{+}CD49b^{-}$ cells. **(A)** Surface expression of CD107a after 4-h stimulation with IL-15. **(B)** Intracellular expression of IFN-γ after 4-h stimulation with IL-15. **(C)** Surface expression of CD107a after 4-h stimulation with IL-12 + IL-18. **(D)** Intracellular expression of IFN-γ after 4-h stimulation with IL-12 + Il-18. Unst. = unstimulated. The bar represents the mean ± SD, symbols represent livers from individual mice, groups consisted of 5-8 mice. One-way analysis of variance (ANOVA), with Tukey's multiple comparisons test. The experiment was performed once.

Supplementary Figure 6. Single-cell RNA-sequencing reveals novel transcriptional signatures of cNKs in the hepatic metastatic niche.

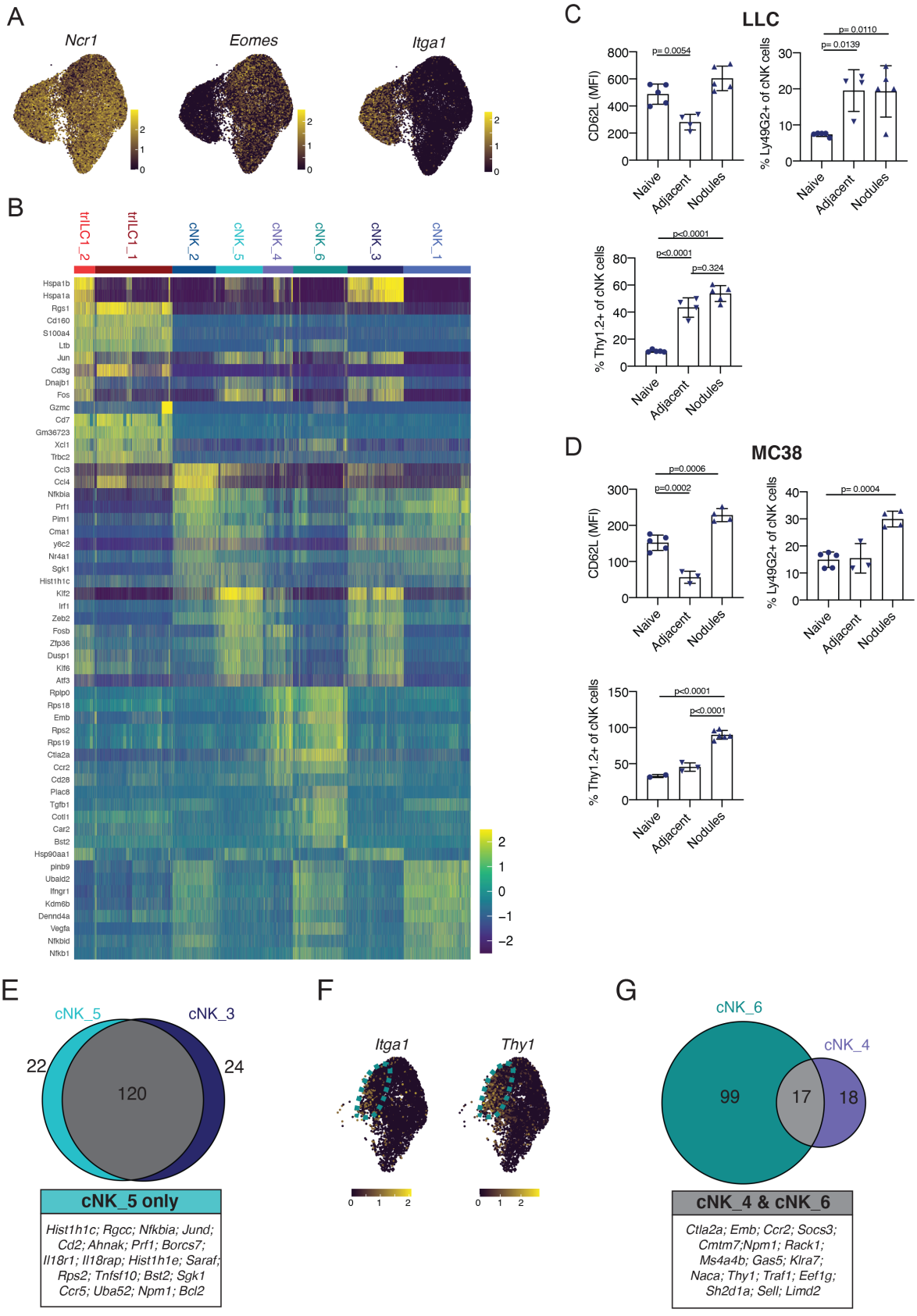

Supplementary Figure 6. Single-cell RNA-sequencing reveals novel transcriptional signatures of cNKs in the hepatic metastatic niche.

Single-cell RNA-sequencing was performed on NKp46^{+} cells sorted from naïve, LLC-metastatic and MC38-metastatic livers (6 mice per condition, pooled into 1 sample for droplet encapsulation and library preparation). **(A)** UMAP analysis of all NKp46^{+} cells with overlaid expression of key lineage markers: NKp46 (*Ncr1*), CD49a (*Itga1*) and Eomes (*Eomes*). **(B)** Heatmap showing the expression of the top-10 genes for each cluster. Cells are plotted in columns and grouped by cluster, and the genes are plotted in rows. **(C, D)** Naïve and metastatic livers were collected. Metastatic livers (day 21) were manually dissected to separate the nodules from the adjacent tissue, and tissues were enzymatically processed into a single-cell suspension. NKp46^{+} cells were analyzed by flow cytometry. Expression of CD62L^{+}, Thy1.2^{+} and Ly49G2^{+} by hepatic cNKs. **(C)** LLC-metastatic liver. **(D)** MC38-metastatic liver. The bar represents the mean ± SD, symbols represent livers from individual mice, groups consisted of 2-6 mice. One-way analysis of variance (ANOVA), with Tukey's multiple comparisons test. The experiment was performed twice with similar results. **(E)** Venn diagram showing differentially expressed genes (DEG) in clusters cNK_3 and cNK_5. The box shows the list of genes exclusive to cNK_5. **(F)** UMAP analysis of cNKs from MC38-metastatic livers with overlaid expression of CD49a (*Itga1*) and Thy1.2 (*Thy1*). The dotted line marks cluster cNK_6. **(G)** Venn diagram showing the differentially expressed genes in clusters cNK_4 and cNK_6. The box shows the list of genes shared by both clusters.

Supplementary Figure 7. TGF-β modulates the fate of CD49a^{+}Eomes^{+} cNKs in metastatic nodules.

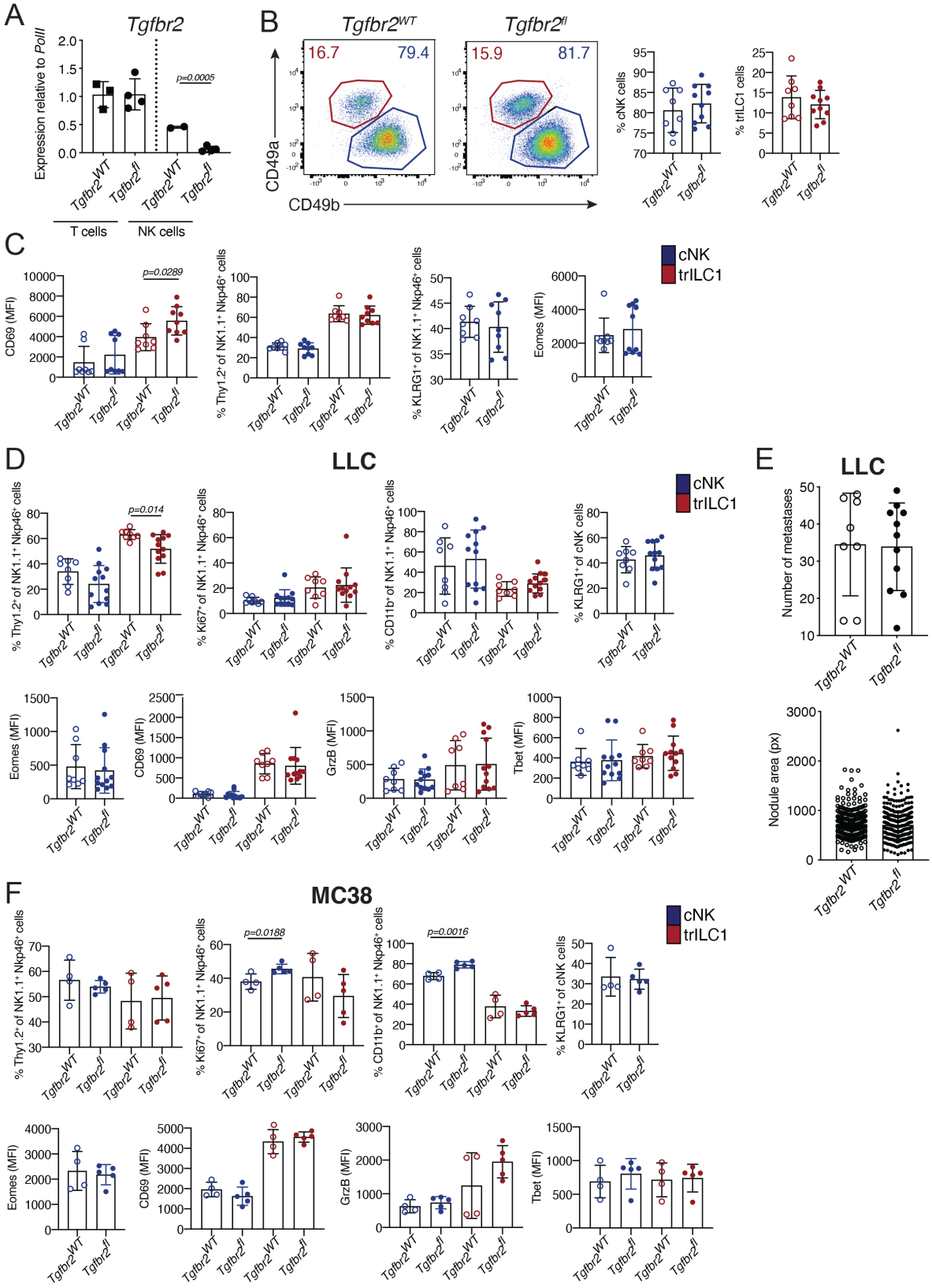

Supplementary Figure 7. TGF-β modulates the fate of CD49a^{+}Eomes^{+} cNKs in metastatic nodules.

(A) Expression of *Tgfbr2* transcripts by T and NKp46^{+} cells sorted from naïve livers. *Tgfbr2^{WT}* = *Ncr1$^{iCre/wt}$.Tgfbr2$^{wt/wt}$*; *Tgfbr2^{fl}* = *Ncr1$^{iCre/wt}$.Tgfbr2$^{fl/fl}$*. **(B)** Representative dot plots and quantification of cNKs and trILC1s in naïve livers of *Tgfbr2^{WT}* and *Tgfbr2^{fl}* mice. Samples were gated on single, live, CD45^{+}lin^{-}NK1.1^{+}NKp46^{+}cells. cNK = conventional NK cells, CD49a^{-}CD49b^{+}; trILC1 = tissue-resident ILC1s, CD49a^{+}CD49b^{-}. The bar represents the mean ± SD, symbols represent livers from individual mice, groups consisted of 8-10 mice. Unpaired Student's t-test. **(C)** Expression of CD69, Thy1.2, KLRG1 and Eomes by cNKs (blue) and trILC1s (red) from naïve livers. *Tgfbr2^{WT}* = *Ncr1$^{iCre/wt}$.Tgfbr2$^{wt/wt}$*; *Tgfbr2^{fl}* = *Ncr1$^{iCre/wt}$.Tgfbr2$^{fl/fl}$*. The bar represents the mean ± SD, symbols represent livers from individual mice, groups consisted of 8-9 mice. One-way analysis of variance (ANOVA), with Tukey's multiple comparisons test. **(D)** LLC-metastatic livers. Upper panels: Proportion of cells expressing Thy1.2^{+}, Ki67^{+}, CD11b^{+} or KLRG1^{+}. Lower panels: Expression of Eomes, CD69, GrzB or Tbet expression in cNKs (blue) and trILC1s (red) from metastatic livers. *Tgfbr2^{WT}* = *Ncr1$^{iCre/wt}$.Tgfbr2$^{wt/wt}$*; *Tgfbr2^{fl}* = *Ncr1$^{iCre/wt}$.Tgfbr2$^{fl/fl}$*. The bar represents the mean ± SD, symbols represent livers from individual mice, groups consisted of 8-12 mice. One-way analysis of variance (ANOVA), with Tukey's multiple comparisons test. **(E)** Quantification of macroscopic LLC liver nodules (number and area) from *Tgfbr2^{WT}* and *Tgfbr2^{fl}* mice 21 days after tumor cell injection. Bars show the mean ± SD. Each symbol represents an individual mouse. One-way analysis of variance (ANOVA), with Tukey's multiple comparisons test. The experiment was performed twice with similar results. **(F)** MC38-metastatic livers. Upper panels: Proportion of cells expressing Thy1.2^{+}, Ki67^{+}, CD11b^{+} or KLRG1^{+}. Lower panels: Expression of Eomes, CD69, GrzB or Tbet expression in cNKs (blue) and trILC1s (red) from metastatic livers. *Tgfbr2^{WT}* = *Ncr1$^{iCre/wt}$.Tgfbr2$^{wt/wt}$*; *Tgfbr2^{fl}* = *Ncr1$^{iCre/wt}$.Tgfbr2$^{fl/fl}$*. The bar represents the mean ± SD, symbols represent livers from individual mice, groups consisted of 4-5 mice. One-way analysis of variance (ANOVA), with Tukey's multiple comparisons test.

Supplementary Table 1

trILC1_1			trILC1_2		cNK_1			cNK_2			cNK_3			cNK_4			cNK_5			cNK_6		
gene	p_val	avg_logFC	gene	p_val	avg_logFC	gene	p_val	avg_logFC	gene	p_val	avg_logFC	gene	p_val	avg_logFC	gene	p_val	avg_logFC	gene	p_val	avg_logFC	gene	p_val	avg_logFC
Cd3g	0	1.6244	*Hspa1b*	0	1.3944	*Prf1*	0	0.6108	*Ccl3*	0	1.1094	*Hspa1a*	0	1.9683	*Emb*	1.4E-250	0.5349	*Klf2*	0	1.1708	*Ctla2a*	0	0.9929
Rgs1	0	1.4893	*Hspa1a*	0	1.2469	*Serpinb9*	0	0.6096	*Ccl4*	0	1.0389	*Hspa1b*	0	1.7944	*Fosb*	7.4E-179	0.5275	*Fos*	0	0.7854	*Emb*	0	0.8557
Gzmc	0	1.0602	*Rgs1*	0	1.0219	*Ubald2*	0	0.5878	*Nfkbia*	0	0.6404	*Klf2*	0	0.8897	*Ctla2a*	2.0E-170	0.5273	*Irf1*	0	0.6834	*Plac8*	0	0.8522
S100a4	0	1.0595	*Dnajb1*	2.1E-257	1.0105	*Ifngr1*	0	0.5402	*Prf1*	0	0.5645	*Fos*	0	0.8117	*Fos*	8.8E-157	0.4433	*Zeb2*	0	0.6442	*Gzmc*	1.8E-23	0.7968
Cd160	0	1.0065	*Jun*	1.0E-277	0.9694	*Kdm6b*	0	0.5225	*Ly6c2*	1.5E-161	0.4780	*Dnajb1*	0	0.7946	*Cd28*	1.5E-141	0.4272	*Fosb*	0	0.6208	*Tgfb1*	0	0.5893
Cd7	0	0.9202	*Cd160*	0	0.9236	*Dennd4a*	0	0.5012	*Sgk1*	1.1E-156	0.4383	*Jun*	0	0.7026	*Ccr2*	3.2E-152	0.4218	*Atf3*	1.1E-156	0.5998	*Ccr2*	0	0.5689
Gm36723	0	0.8701	*Cd3g*	6.7E-267	0.8895	*Vegfa*	0	0.4724	*Cma1*	5.7E-209	0.4364	*Atf3*	2.7E-210	0.6629	*Rack1*	1.2E-194	0.3314	*Zfp36*	0	0.5331	*Cotl1*	0	0.5369
Xcl1	0	0.8672	*Fos*	2.7E-215	0.8593	*Nfkbid*	2.6E-292	0.4300	*Nr4a1*	3.5E-161	0.4173	*Zeb2*	0	0.5890	*Sh2d1a*	4.1E-136	0.3279	*Dusp1*	5.8E-303	0.5207	*Bst2*	2.8E-218	0.5318
Ltb	0	0.8355	*S100a4*	0	0.7820	*Nfkb1*	3.2E-246	0.3860	*Pim1*	1.2E-252	0.4168	*Hsp90aa1*	0	0.5376	*Klra7*	1.1E-32	0.3151	*Sgk1*	1.0E-129	0.4821	*Car2*	0	0.5229
Trbc2	0	0.8266	*Ltb*	0	0.7586	*Ly6c2*	1.2E-146	0.3750	*Hist1h1c*	5.7E-81	0.3780	*Klf6*	0	0.5173	*Klf4*	7.6E-97	0.3086	*Klf6*	3.9E-292	0.4659	*Prdx6*	0	0.5204
Osgin1	0	0.7474	*Cd7*	0	0.7302	*Id2*	8.1E-251	0.3707	*Klra9*	2.3E-100	0.3776	*Dusp1*	2.8E-277	0.4947	*Npm1*	1.2E-75	0.2939	*Cma1*	7.1E-286	0.4608	*Pmepa1*	0	0.4944
Gzmb	0	0.7443	*Gm36723*	0	0.7164	*Gzma*	1.8E-296	0.3673	*Dusp2*	1.2E-95	0.3748	*Dnaja1*	1.9E-196	0.4771	*Naca*	8.6E-107	0.2742	*Ly6c2*	5.9E-123	0.4373	*Vegfa*	0	0.4826
Itga1	0	0.7070	*Rgs2*	4.1E-160	0.6949	*Serpinb6b*	3.9E-152	0.3672	*Icam1*	1.4E-117	0.3633	*Fosb*	5.8E-203	0.4648	*Limd2*	4.6E-80	0.2688	*Hist1h1c*	2.1E-94	0.4182	*Smad7*	0	0.4807
Ly6e	0	0.6577	*Cited4*	3.2E-243	0.6761	*Nfkbia*	2.4E-254	0.3482	*Gzma*	1.7E-207	0.3557	*Irf1*	7.2E-205	0.4509	*Vim*	3.2E-37	0.2627	*Jun*	1.2E-233	0.4177	*Socs3*	0	0.4636
Il21r	0	0.6394	*Trbc2*	1.3E-188	0.6401	*Bcl2a1b*	1.8E-101	0.3477	*Nfkbid*	8.0E-118	0.3517	*Ifng*	4.1E-96	0.4436	*Pycard*	1.5E-55	0.2487	*Btg2*	1.6E-257	0.4002	*Cxcr4*	0	0.4593
Ckb	0	0.5931	*Cxcr3*	0	0.6230	*Dusp2*	9.0E-178	0.3445	*Lgals1*	5.8E-162	0.3265	*Hspa8*	1.8E-269	0.4392	*Hspe1*	1.2E-55	0.2484	*Rhob*	8.1E-174	0.3897	*Runx3*	6.6E-272	0.4538
Rgs2	0	0.5789	*Dnaja1*	6.6E-113	0.5712	*Orai1*	1.5E-183	0.3442	*Gadd45b*	4.3E-44	0.3157	*Ly6c2*	1.2E-162	0.4166	*Gas5*	7.7E-71	0.2441	*Ier2*	1.1E-227	0.3756	*Cmtm7*	0	0.4293
Trbc1	0	0.5779	*Hsph1*	1.8E-196	0.5519	*Btg1*	3.7E-288	0.3373	*Emp3*	6.7E-170	0.3030	*Zfp36*	5.3E-186	0.4040	*Sell*	8.4E-63	0.2433	*Egr1*	3.1E-106	0.3690	*Gramd3*	0	0.4274
Nedd9	0	0.5756	*Cd226*	0	0.5454	*Ccl5*	1.5E-276	0.3328	*Nfkbiz*	3.0E-98	0.3029	*Rhob*	4.6E-166	0.3793	*Cmtm7*	6.0E-66	0.2344	*Icam1*	2.2E-86	0.3601	*Npm1*	1.6E-251	0.4256
Cd226	0	0.5738	*Ly6e*	9.9E-229	0.5333	*Sh2d2a*	6.1E-210	0.3306	*Ubald2*	3.6E-122	0.2946	*Klra4*	2.8E-128	0.3755	*Actb*	1.2E-40	0.2290	*Ifng*	7.0E-67	0.3595	*Rack1*	0	0.4255
Klrc1	0	0.5694	*Hsp90aa1*	3.4E-136	0.5254	*Rap1b*	1.2E-270	0.3256	*Bhlhe40*	1.9E-131	0.2915	*Ubc*	3.5E-215	0.3644	*Ms4a4b*	7.1E-63	0.2251	*Ccl3*	2.6E-107	0.3517	*Ms4a4b*	3.7E-253	0.4230
Ccl4	1.3E-257	0.5503	*Klf6*	5.9E-148	0.5235	*Cma1*	1.0E-215	0.3180	*Klrg1*	1.1E-138	0.2792	*Hsp90ab1*	2.8E-258	0.3522	*Irf1*	7.0E-34	0.2217	*Rgcc*	6.4E-72	0.3459	*Stat3*	7.6E-242	0.4084
S100a6	0	0.5479	*Klrc1*	1.0E-148	0.5086	*Irf8*	0	0.3146	*Serpinb9*	2.4E-90	0.2699	*Cma1*	1.9E-201	0.3360	*Hsp90ab1*	4.3E-53	0.2199	*Vim*	1.6E-170	0.3383	*Shisa5*	0	0.4059
Cxcr3	0	0.5165	*Dusp1*	7.1E-93	0.5074	*Cd9*	5.3E-189	0.3116	*Klra8*	1.5E-49	0.2653	*Egr1*	4.1E-83	0.3295	*Egr1*	9.4E-34	0.2163	*Gm26532*	2.1E-147	0.3317	*Gas5*	2.7E-270	0.3943
Stk17b	0	0.5001	*Ckb*	0	0.5072	*Ppig*	3.5E-133	0.3084	*Rap1b*	2.5E-122	0.2569	*Ier5*	5.1E-170	0.3184	*Hspa8*	1.8E-53	0.2157	*Neat1*	2.3E-102	0.3144	*Aldoa*	1.0E-119	0.3850
Irf1	5.4E-209	-0.5458	*Emp3*	7.6E-113	-0.4676	*S100a4*	1.9E-114	-0.5067	*Cxcr3*	3.2E-138	-0.3255	*Osgin1*	1.2E-162	-0.3622	*Il21r*	2.1E-53	-0.2789	*Mpp7*	4.9E-110	-0.3370	*Emp3*	1.2E-240	-0.4158
Ctla2a	9.4E-162	-0.5505	*Vim*	1.6E-89	-0.4709	*Dusp1*	5.9E-149	-0.5192	*Serpina3g*	6.9E-96	-0.3486	*Srgn*	1.6E-268	-0.3671	*Btg1*	1.9E-76	-0.2797	*Smad7*	6.6E-111	-0.3463	*Sgk1*	3.8E-81	-0.4389
Eomes	0	-0.5524	*Ctla2a*	1.0E-53	-0.4902	*Btg2*	0	-0.5248	*Klf6*	2.3E-63	-0.3626	*Serpinb9*	9.8E-99	-0.3673	*Ubald2*	1.2E-32	-0.2893	*Tgfb1*	4.1E-100	-0.3497	*Klra9*	2.1E-117	-0.4677
Cd2	0	-0.5751	*Sell*	4.5E-139	-0.5024	*Ccl4*	3.4E-30	-0.5383	*Trbc1*	4.6E-123	-0.3770	*Ccl4*	9.5E-43	-0.3674	*Hist1h1c*	2.2E-16	-0.2966	*Osgin1*	8.4E-140	-0.3575	*Zeb2*	3.9E-150	-0.4781
Anxa2	0	-0.5789	*Anxa2*	1.2E-171	-0.5237	*Xcl1*	1.2E-163	-0.5419	*Rgs2*	1.3E-74	-0.3880	*Litaf*	4.1E-206	-0.3679	*Srgn*	2.2E-99	-0.2970	*Litaf*	1.9E-157	-0.3614	*Dnaja1*	6.4E-166	-0.4800
Sell	0	-0.5861	*Pim1*	7.0E-144	-0.5822	*Zfp36*	2.0E-301	-0.5741	*Xcl1*	5.9E-77	-0.4070	*Tgfb1*	5.3E-141	-0.3726	*Osgin1*	6.4E-64	-0.3035	*Gzmb*	1.2E-20	-0.3652	*S100a6*	6.2E-193	-0.4903
Emp3	0	-0.5972	*Itga4*	1.8E-148	-0.5974	*Ly6e*	0	-0.5769	*Gm36723*	1.6E-136	-0.4309	*Neurl3*	7.5E-139	-0.3745	*Klra9*	5.7E-33	-0.3312	*Hspa1b*	1.8E-17	-0.3687	*Ccl5*	0	-0.5124
Ms4a4b	0	-0.6070	*Kdm6b*	8.9E-132	-0.6119	*Cd69*	5.9E-281	-0.6065	*Ctla2a*	4.5E-64	-0.4401	*Smad7*	9.3E-153	-0.3848	*Cma1*	8.5E-45	-0.3348	*Trbc1*	1.9E-127	-0.3707	*Gzma*	2.3E-290	-0.5321
Vim	0	-0.6409	*Serpinb9*	2.8E-126	-0.6149	*Klf2*	1.3E-41	-0.6281	*Emb*	1.0E-102	-0.4489	*Dusp5*	5.4E-207	-0.3990	*Dennd4a*	1.7E-104	-0.3838	*Emb*	1.1E-61	-0.3729	*S100a4*	6.8E-137	-0.5401
Itga4	0	-0.7057	*Sgk1*	4.4E-90	-0.6165	*Cd160*	6.0E-254	-0.6446	*Trbc2*	6.4E-92	-0.4890	*Trbc1*	6.2E-171	-0.3998	*S100a4*	3.9E-40	-0.3872	*Ppp1r16b*	1.1E-164	-0.3798	*Klf6*	5.7E-251	-0.5619
Lgals1	0	-0.7561	*Klf2*	1.8E-47	-0.6212	*Ifng*	1.4E-154	-0.6457	*Cd7*	1.7E-165	-0.5035	*Dennd4a*	1.2E-204	-0.4063	*Xcl1*	4.8E-16	-0.4006	*Gm36723*	4.0E-149	-0.4366	*Cma1*	2.1E-241	-0.5886
Klra13-ps	0	-0.7580	*Klra13-ps*	1.2E-121	-0.6315	*Ccl3*	1.5E-44	-0.7037	*S100a4*	1.2E-85	-0.5073	*Bcl2a1b*	6.2E-116	-0.4329	*Serpinb9*	7.3E-64	-0.4076	*Prdx6*	1.2E-180	-0.4464	*Btg2*	0	-0.5891
Sgk1	0	-0.7668	*Gzma*	6.1E-148	-0.6332	*Klf6*	0	-0.7241	*Fosb*	7.3E-121	-0.5273	*Trbc2*	7.5E-87	-0.4436	*Bcl2a1b*	7.5E-70	-0.4348	*Trbc2*	6.0E-79	-0.4477	*Dusp1*	6.9E-284	-0.6394
Klra7	0	-0.7740	*Klra7*	5.1E-91	-0.6437	*Ltb*	0	-0.7453	*Dnajb1*	1.2E-79	-0.5483	*Cd7*	2.8E-146	-0.4456	*Gzma*	7.3E-125	-0.4483	*Bcl2a1b*	6.8E-117	-0.4627	*Ly6c2*	8.4E-183	-0.6950
Zeb2	0	-0.8126	*Ubald2*	1.1E-156	-0.6485	*Dnajb1*	9.4E-183	-0.7537	*Ly6e*	4.2E-228	-0.5667	*Gm36723*	3.7E-179	-0.4477	*Prf1*	4.5E-76	-0.4488	*Cd7*	6.9E-146	-0.4666	*Jun*	1.9E-195	-0.7015
Cma1	0	-0.8313	*Zeb2*	5.8E-151	-0.6502	*Atf3*	1.5E-170	-0.7668	*Cd160*	1.5E-155	-0.6115	*Prdx6*	1.2E-266	-0.4920	*Neurl3*	2.7E-111	-0.4535	*S100a4*	2.6E-86	-0.5067	*Rgs1*	4.6E-94	-0.7928
Hspa1b	6.5E-69	-0.9003	*Lgals1*	2.6E-192	-0.6955	*Fosb*	0	-0.8091	*Ltb*	2.9E-233	-0.6992	*Ly6e*	6.3E-229	-0.5094	*Ccl3*	9.9E-33	-0.4703	*Ly6e*	1.2E-191	-0.5116	*Cd3g*	7.8E-65	-0.7928
Ly6c2	0	-0.9357	*Cma1*	5.8E-148	-0.7088	*Gzmc*	9.4E-103	-0.8812	*Jun*	1.9E-107	-0.7451	*S100a4*	8.6E-114	-0.5329	*Ly6c2*	1.2E-49	-0.4725	*Cd160*	1.4E-164	-0.6089	*Dnajb1*	1.2E-230	-0.7980
Nfkbia	0	-0.9376	*Ifngr1*	3.3E-254	-0.7537	*Cd3g*	5.9E-169	-1.0074	*Gzmc*	1.8E-58	-0.8379	*Cd160*	5.1E-158	-0.5788	*Dusp2*	1.7E-122	-0.5391	*Ltb*	1.2E-245	-0.6932	*Ccl4*	0	-0.9348
Hspa1a	4.8E-94	-1.0335	*Ly6c2*	1.5E-77	-0.7759	*Rgs1*	3.7E-220	-1.0897	*Cd3g*	1.8E-107	-0.9705	*Ltb*	3.7E-261	-0.6604	*Cd3g*	5.0E-23	-0.6583	*Rgs1*	4.3E-58	-0.7234	*Fos*	2.0E-199	-0.9525
Klra8	0	-1.0413	*Klra8*	7.9E-122	-0.8485	*Jun*	0	-1.4354	*Rgs1*	2.2E-153	-1.0460	*Xcl1*	2.6E-206	-0.6623	*Gzmc*	3.5E-20	-0.7619	*Xcl1*	8.4E-235	-0.8050	*Klf2*	4.2E-288	-1.0461
Prf1	0	-1.1552	*Nfkbia*	5.5E-252	-0.9858	*Fos*	0	-1.4808	*Fos*	1.1E-170	-1.0618	*Rgs1*	3.0E-60	-0.6642	*Rgs1*	1.9E-75	-0.8273	*Hspa1a*	1.1E-13	-0.8416	*Ccl3*	0	-1.1192
Klra4	0	-1.3735	*Prf1*	2.9E-297	-1.1014	*Hspa1a*	8.9E-266	-1.6612	*Hspa1a*	9.0E-129	-1.4165	*Gzmc*	1.0E-87	-0.8657	*Ccl4*	6.4E-136	-0.8537	*Gzmc*	9.0E-66	-0.8481	*Hspa1a*	8.0E-208	-1.4513
Klf2	0	-1.5987	*Klra4*	5.6E-175	-1.1675	*Hspa1b*	0	-1.9922	*Hspa1b*	8.2E-167	-1.5368	*Cd3g*	6.9E-135	-0.9767	*Gzmb*	1.9E-266	-0.9324	*Cd3g*	3.6E-124	-0.9860	*Hspa1b*	0	-1.6418

Supplementary Table 1: Top 25 upregulated genes and downregulated genes for each trILC1 and cNK cluster identified from scRNA. p_val = p value, avg_logFC = average log2 (Fold Change).